⌘ *Author's Choice*

THE JOURNAL OF BIOLOGICAL CHEMISTRY VOL. 287, NO. 50, pp. 42093–42103, December 7, 2012

Characterization of Streptokinases from Group A Streptococci Reveals a Strong Functional Relationship That Supports the Coinheritance of Plasminogen-binding M Protein and Cluster 2b Streptokinase*[S]

Received for publication, September 7, 2012, and in revised form, October 9, 2012 Published, JBC Papers in Press, October 18, 2012, DOI 10.1074/jbc.M112.417808

Yueling Zhang, Zhong Liang, Hsing-Tse Hsueh, Victoria A. Ploplis, and Francis J. Castellino[1]

From the W. M. Keck Center for Transgene Research and Department of Chemistry and Biochemistry, University of Notre Dame, Notre Dame, Indiana 46556

Background: GAS virulence is dependent on a functional human fibrinolytic system.
Results: Functional differences between different strains of GAS streptokinases have been found.
Conclusion: Pressure on coinheritance of specific GAS streptokinases and M proteins is identifiable.
Significance: Tissue tropism and virulence of GAS infections are reflected in the types of streptokinases and M proteins.

Group A streptococcus (GAS) strains secrete the protein streptokinase (SK), which functions by activating host human plasminogen (hPg) to plasmin (hPm), thus providing a proteolytic framework for invasive GAS strains. The types of SK secreted by GAS have been grouped into two clusters (SK1 and SK2) and one subcluster (SK2a and SK2b). SKs from cluster 1 (SK1) and cluster 2b (SK2b) display significant evolutionary and functional differences, and attempts to relate these properties to GAS skin or pharynx tropism and invasiveness are of great interest. In this study, using four purified SKs from each cluster, new relationships between plasminogen-binding group A streptococcal M (PAM) protein and SK2b have been revealed. All SK1 proteins efficiently activated hPg, whereas all subclass SK2b proteins only weakly activated hPg in the absence of PAM. Surface plasmon resonance studies revealed that the lower affinity of SK2b to hPg served as the basis for the attenuated activation of hPg by SK2b. Binding of hPg to either human fibrinogen (hFg) or PAM greatly enhanced activation of hPg by SK2b but minimally influenced the already effective activation of hPg by SK1. Activation of hPg in the presence of GAS cells containing PAM demonstrated that PAM is the only factor on the surface of SK2b-expressing cells that enabled the direct activation of hPg by SK2b. As the binding of hPg to PAM is necessary for hPg activation by SK2b, this dependence explains the coinherant relationship between PAM and SK2b and the ability of these particular strains to generate the proteolytic activity that disrupts the innate barriers that limit invasiveness.

Group A *Streptococcus* is a strictly human pathogen that is responsible for >600 million cases of superficial and treatable pharyngitis annually and an additional >100 million cases annually of impetigo and related skin disorders (1). In more rare cases, these bacteria also cause life-threatening invasive infections such as toxic shock syndrome, necrotizing fasciitis, and myositis (2). Based on the diversity of a ubiquitous cell wall-anchored virulence-determinant M protein and M-like protein encoded by *emm* genes (3), >250 types of GAS[2] have been identified (4). Decades of studies have revealed numerous GAS pathogenic mechanisms that rely on specific bacterial product interactions with human proteins (5–9), among which host human plasminogen (hPg) has been shown to be used by GAS as a critical virulence factor, especially in invasive skin-tropic strains of these bacteria. hPg activation by GAS not only would provide a proteolytic framework for invasive mechanisms of GAS but would also lead specifically to accelerated clearance of host fibrin, which encapsulates GAS and thereby limits bacterial invasion and spread (10, 11).

The activity of the human fibrinolytic system is primarily dependent on the activation of the circulating zymogen, hPg, to the serine protease, human plasmin (hPm). This latter enzyme catalyzes clot degradation by limited proteolytic cleavage of fibrin. The activation of hPg requires proteolytic cleavage of the Arg^{561}–Val^{562} peptide bond in the single chain hPg zymogen, thus generating the disulfide-linked two-chain serine protease, hPm (12). Therefore, the major hPg activators of mammalian origin, *viz.* urokinase-type plasminogen activator and tissue-type plasminogen activator, are in themselves proteases capable of highly specific cleavage of the requisite peptide bond in hPg.

A different hPg activation system exists in bacterial systems, where the main hPg activators are exoproducts of the bacteria, which in some strains are most effective when hPg is bound to bacterial receptors. Specifically, in GAS, the main hPg activator is the secreted protein streptokinase (SK). The mechanism of activation of hPg to hPm by SK is unique in that SK is not a

* This work was supported, in whole or in part, by National Institutes of Health Grant HL013423.
⌘ *Author's Choice*—Final version full access.
[S] This article contains supplemental Fig. 1 and Tables 1 and 2.
The nucleotide sequence(s) reported in this paper has been submitted to the GenBank™/EBI Data Bank with accession number(s) JX898180–JX898186
[1] To whom correspondence should be addressed. Tel.: 574-631-9152; E-mail: fcastell@nd.edu.

[2] The abbreviations used are: GAS, group A *Streptococcus*; hPg, human plasminogen; hPm, human plasmin; hFg, human fibrinogen; SK, streptokinase; RU, response unit; RC, reverse-complemented; EACA, ϵ-aminocaproic acid; PAM, plasminogen-binding group A streptococcal M.

protease and thus is incapable of directly cleaving the single peptide bond required for hPg activation. To overcome this defect, SK forms a complex with hPg that conformationally generates an active site that strictly functions to activate hPg to hPm (13). A mechanistic feature of many strains, wherein the bacterial SK employs host receptor-bound hPg to generate a protease that also binds to GAS receptors, primarily of the M protein class, allows the specific GAS strains to assemble a proteolytic surface that functions to degrade barriers to the dissemination of GAS, *e.g.* fibrin and extracellular matrix proteins, and also serves to protect hPm from inactivation by the host inhibitor α2-antiplasmin. Some invasive strains of GAS assemble hPg/hPm directly on a surface-exposed plasminogen-binding group A streptococcal M (PAM) protein and PAM-like proteins (14), whereas other GAS strains employ distinct surface M proteins (*e.g.* M1) to bind host human fibrinogen (hFg), which in turn interacts with hPg/hPm (15). The importance of hPg in the virulence of GAS has been demonstrated eloquently in mice containing an hPg transgene, which show greatly enhanced GAS virulence as compared with wild-type (WT) mice (10). Endogenous mouse plasminogen is highly resistant to activation by SK from GAS.

SK alleles from GAS are polymorphic and have been classified into two clusters (SK1 and SK2) and at least one subcluster (SK2a and SK2b) (16, 17). Detailed genetic and epidemiological investigations of more than 90 GAS strains have revealed that all strains harboring the *sk1* allele lacked PAM, whereas all of the PAM-positive strains had a *sk2b* allele. This strongly suggests that there is a coinherant relationship between sk2b and pam-expressing GAS strains and that the combination of sk2b and pam might play a key role in skin tissue tropism and strain invasiveness (16). Although these findings propose a strong coselective pressure behind the alleles, the functional effects resulting from this selective pressure remain unknown. It has been shown that there are significant functional differences between SK1 and SK2b (17), but the role of PAM in hPg activation by SK2b has not been identified. Considering the strong coinheritance between PAM and SK2b, we attempted to identify the functional relationships between PAM and SK2b with regard to hPg activation using purified proteins cloned and expressed from primary GAS isolates of throat and skin infections. The results of these studies have identified the functional relationships between PAM and SK2b on hPg activation.

EXPERIMENTAL PROCEDURES

Bacterial Strains—WT GAS primary isolate strains NS210, NS53, NS931, NZ131, AP53, NS223, NS455, and NS88.2, as well as mutant strains NS88.2/*prp* and NS88.2/*prp*RC, were gifts from Dr. Mark J. Walker (Queensland, Australia). GAS strain AP53 was donated by Dr. Gunnar Lindahl (Lund, Sweden). GAS strain SF370 was purchased from the American Type Culture Collection. These strains were cultured on defibrinated sheep blood plates or in Todd-Hewitt broth (BD Bacto, Franklin Lakes, NJ) supplemented with 1% (w/v) yeast extract (THY) (BD Bacto) at 37 °C, 5% CO_2.

The AP53/Δ*pam* mutant strain was constructed by an allelic replacement of *pam* with chloramphenicol transferase (*cat*) employing previously described methodology (18). Using PCR, a 282-bp fragment upstream of the *pam* gene was amplified with the primers *pam*5F-NotI and *pam*5R (supplemental Table 1). Additionally, a 281-bp fragment downstream of the *pam* gene was amplified using *pam*3F and *pam*3R-SalI (supplemental Table 1). The primers adjacent to *pam* contained a 20-bp overhang of the *cat* gene corresponding to the upstream and downstream ends of *cat*, respectively.

The upstream and downstream fragments were combined with the 660-bp *cat* gene in a fusion PCR using primers *pam*5F-NotI and *pam*3R-SalI. This triple fragment was T-A-cloned in pCR2.1-TOPO (Invitrogen) and digested using restriction enzymes NotI and SalI. The resulting fragment was ligated into the NotI- and SalI-digested temperature-sensitive vector pHY304 to generate the knock-out plasmid pHY*pam*-KO. WT AP53 cells were then transformed with pHY*pam*-KO electroporation. Chromosomal integration via allelic replacement was achieved by a single crossover (SCO) at 30 °C for 2 h for plasmid replication and then switched to 37 °C overnight for screening for erythromycin resistance (em^R). SCO^+ mutants were confirmed by PCR with primers internal to the em^R gene. For the double crossover (DCO), the confirmed SCO^+ cells were replicated at 30 °C overnight and then switched to 37 °C overnight, both without erythromycin. Finally, screening for erythromycin-sensitive colonies was used to identify DCO^+ mutants. Allelic replacement was confirmed by PCR. An in-frame allelic replacement *pam* mutant, AP53/Δ*pam*, was confirmed by multiple PCR reactions showing the insertion of the *cat* gene and the absence of the *pam* gene in the genome.

Expression Plasmids—Streptokinase genomic DNAs (gDNA) from primary isolates, *viz*. NS210, NS53, NS931, NZ131, AP53, NS223, NS455, NS88.2, and SF370, were extracted using standard methodology for Gram-positive bacteria (19). Because the full *sk* gene sequences in most of these strains were unknown, in order to clone the *sk* genes, primers *sk*F and *sk*R (supplemental Table 1) were designed by alignment of the *sk* gene flanking sequences from known genomic sequences of *Streptococcus pyogenes* strains NZ131 (NC_011375), M1GAS (NC_002737), MGAS5005 (NC_007297), MGAS6180 (NC_007296), and MGAS10270 (NC008022). With the genomic DNA as a template, full-length *sk* genes from all of these strains, with 32 bp of upstream and 62 bp of downstream *sk* open reading frame sequences, were amplified by primers *sk*F and *sk*R (supplemental Table 1). The PCR products were cloned into pCR2.1-TOPO (Invitrogen) and sequenced.

To construct *sk* expression plasmids, primers (supplemental Table 1) were designed to amplify the coding sequences for 414 residues, encompassing residues 1–414, without the 26-amino acid (−26 to −1) signal peptide, for each *sk* gene. All of the reverse primers included introduction of a BamHI site. PCR was carried out with Phusion Hot Start high-fidelity DNA polymerase (New England Biolabs, Ipswich, MA). After digestion by BamHI, the PCR products were ligated into PshAI/BamHI-digested pET42a (EMD4Biosciences, Darmstadt, Germany).

To construct the *pam* expression plasmid, the coding sequence for PAM_{AP53} from residues 42–392, without both the signal peptide and the LPXTG cell membrane insertion domain, was amplified from GAS AP53 genomic DNA with

primers *pam*F and *pam*R (supplemental Table 1). The latter primer introduces a coding sequence for a His_6 tag at the 3′-end of the *pam* gene for further purification. After double digestion with NcoI and EcoRI, the PCR product was ligated into NcoI/EcoRI-digested pET28a. The same cloning, digestion, and ligation strategy was used to clone the coding sequence for $M1_{SF370}$, from residues 42–449, from GAS SF370 genomic DNA with primers *emm-1*F and *emm-1*R (supplemental Table 1). *Escherichia coli* Top10 (Invitrogen) cells were transformed with the ligation mixtures by electroporation. Clones containing plasmids with the correct inserts of each gene were screened by sequencing.

Full-length $rGlu^1$-hPg, with Glu as the N-terminal amino acid and containing a mutation at the active site serine (S741A) of latent hPm, *viz.* $rGlu^1$-hPg[S741A], was produced with the QuikChange site-directed mutagenesis kit (Stratagene) according to the manufacturer's instructions, using plasmid pMT-PURO as a template (20).

Gene Expression and Protein Purification—To express various rSKs as well as $rPAM_{AP53}$ and $rM1_{SF370}$, *E. coli* BL21/DE3 (New England Biolabs) cells were transformed with the expression plasmids. The overnight culture ($A_{600\,nm} \sim 1.2$) of the transformed cells was inoculated at 1% (v/v) in 1 liter of LB broth plus kanamycin (40 μg/ml) and incubated at 37 °C until an $A_{600\,nm}$ of ~0.6 was reached. Protein expression was induced by the addition of 0.8 mM isopropyl-1-thio-β-D-galactopyranoside, and growth of the cultures was continued for 5 h under these same conditions. The cultures were then centrifuged, and the cell pellets were resuspended in 80 ml of binding buffer (20 mM Tris-HCl, pH 7.9, 0.5 M NaCl, and 20 mM imidazole) with 0.5 mg/ml lysozyme (Ameresco, Solon, OH) and EDTA-free proteinase inhibitor mixture (Roche Applied Science). After incubation at 37 °C for 20 min, the cells were disrupted by sonication, and supernates were collected after centrifugation at 12,000 rpm for 10 min at 4 °C.

The tagged proteins in the supernates collected above were bound to His-Bind resin (EMD4Biosciences) by loading the supernatant at 4 °C onto a column containing nickel-charged His-Bind resin. After the column was washed with binding buffer, the protein was eluted with a solution of 20 mM Tris-HCl, pH 7.9, 0.5 M NaCl, and 250 mM imidazole. In the case of $rPAM_{AP53}$ or $rM1_{SF370}$, the eluate contained purified $rPAM_{AP53}$ or $rM1_{SF370}$ protein. Both proteins included one non-native alanine at the N terminus and six consecutive histidines at the C terminus. The elution buffer was changed to 100 mM sodium phosphate, pH 7.4, using a PD-10 desalting column (GE Healthcare), and the final $rPAM_{AP53}$ and $rM1_{SF370}$ solutions were stored in aliquots at −80 °C for later use.

The above eluted rSKs possess an N-terminal 276-amino acid tag from pET42a, which contains, sequentially, a glutathione sulfur-transferase tag, an S tag, a His_6 tag, and a factor Xa cleavage site. To remove this three-tag fragment, the rSK was incubated with factor Xa at a factor Xa:protein ratio (unit/μg) of 1:200. The protein mixture was then reloaded on a nickel-charged His-Bind column at 4 °C. The highly purified rSK was collected in the flow-through, from which the factor Xa was removed by Xarrest-agarose (EMD4Biosciences). Finally, the buffers of rSK solutions were changed to 10 mM sodium phosphate, pH 7.4, using a PD-10 desalting column. All purified rSK proteins contained 414 residues from residue 27–440 of each SK without non-native residues. Yields of original cultures at ~8–12 mg/liter were obtained.

Human $rGlu^1$-hPg and $rGlu^1$-hPg[S741A] in plasmid pMT-PURO (20) were expressed in *Drosophila* Schneider S2 cells and purified by Sepharose-lysine affinity chromatography as described previously (21). hPgs were obtained at yields of 6–10 mg/liter of culture fluid.

Protein Purity and Concentration Determinations—The purity of $rPAM_{AP53}$ and all eight of the purified SKs were assessed with 12% (w/v) SDS-PAGE. Protein concentrations were measured by the absorbance at 280 nm using the following calculated (Protein Calculator version 3.3) extinction coefficients ($M^{-1}cm^{-1}$): His_6-tagged $rPAM_{AP53}$, 8,250; His_6-tagged $rM1_{SF370}$, 10,810; rSK_{NS210}, 35,130; rSK_{NS53}, 35,130; rSK_{NZ131}, 35,130; rSK_{NS931}, 33,850; rSK_{AP53}, 33,850; rSK_{NS223}, 32,570; rSK_{NS455}, 32,570; and $rSK_{NS88.2}$, 32,570.

Activation of Glu^1-hPg by SK Variants—The activation of $rGlu^1$-hPg by rSK variants was monitored in 96-well microtiter plates using the chromogenic substrate S2251 (*H*-D-Val-Leu-Lys-pNA; Chromogenix, Milan, Italy) to monitor the continual formation of the generated protease, hPm. Each well contained 0.2 μM Glu^1-hPg/0.25 mM S2251 in 200 μl of 10 mM Hepes/150 mM NaCl, pH 7.4. The reaction was accelerated by the addition of 2 μl of 0.5 μM SK. In assays investigating the effects of protein factors and cells on rhPg activation by rSKs, the indicated amount of $rPAM_{AP53}$, hFg (Enzyme Research Laboratories, South Bend, IN), $rM1_{SF370}$, or GAS cells was premixed with substrate S2251 and $rGlu^1$-hPg in 10 mM Hepes/150 mM NaCl, pH 7.4, and the reaction was accelerated by the addition of rSK. The amidolytic activity generated by hPm hydrolysis of substrate S2251 was monitored by continuous measurement of the $A_{405\,nm}$. For more quantitative estimates, the $A_{405\,nm}$, which measures both the activation rate of hPg and also the cleavage of the substrate S2251 by the generated hPm, was also plotted against t^2. The initial velocities were then calculated from the slope of $A_{405\,nm}$ *versus* t^2 and compared. The ratio of initial velocity in the presence and absence of a specific protein or cell of a specific strain was defined as the potentiation factor of the added protein or cells. All data transformations and linear regressions were performed by GraphPad Prism 5.

Surface Plasmon Resonance (SPR)—Association and dissociation rates of rhPg binding to rSK were measured in real time by SPR with a BIAcore X100 Biosensor (GE Healthcare). To avoid activation of hPg during the binding process, a Glu^1-hPg mutant, $rGlu^1$-hPg[S741A], in which the hPm active site Ser^{741} was replaced with Ala, was used. $rGlu^1$-hPg[S741A] was immobilized onto the sensor chip CM-5 (GE Healthcare) using the amine coupling method. For immobilization, 20 μg/ml $rGlu^1$-hPg[S741A] in 10 mM NaOAc, pH 4.5, was used to reach ~1000 response units (RU) for studying the binding kinetics of SK1 (rSK_{NS210}, rSK_{NS53}, rSK_{NS931}, and rSK_{NZ131}) and ~1500 RU to investigate the binding kinetics of SK2b (rSK_{AP53}, rSK_{NS223}, rSK_{NS455}, and $rSK_{NS88.2}$). The flow cell was treated similarly, except that $rGlu^1$-hPg[S741A] was not injected. This was then employed as a control surface for the subtraction of the non-specific binding. Binding kinetics were measured for $rGlu^1$-

hPg[S741A] and each rSK in HBS-EP buffer (10 mM Hepes, 150 mM NaCl, 3 mM EDTA, and 0.005% P20, pH 7.4). Concentrations from 1 to 50 nM were used for SK1 and from 10 to 500 nM for SK2b. The analytes were injected at a flow rate of 50 μl/min for 90 s. Post-injection phase dissociation was monitored in the running buffer for 120 s. The surface was regenerated between injections using 35 mM NaOH at a flow rate of 50 μl/min for 30 s. The background was subtracted by passing the protein solution over the control surface. The kinetic constants were calculated from the sensorgrams by nonlinear fitting of the association and dissociation curves according to a 1:1 binding model using BIAevaluation software 4.1 (GE Healthcare).

GAS Cell Preparations—To study hPg binding by cells and the functions of cells in rGlu^1-hPg activation by rSK, the cells of WT GAS strains, *viz.* NS210, NS53, NS931, NZ131, AP53, NS223, NS455, and NS88.2, as well as the mutant strains AP53/Δ*pam*, NS88.2/*prp*, and NS88.2/*prpRC,* were prepared as follows. Single colonies of each strain were inoculated in THY medium to grow overnight at 37 °C, and this overnight culture ($A_{600\ nm}$ = 1.1–1.3) was inoculated (1%, v:v) in prewarmed THY medium to reach an $A_{600\ nm} \sim 0.6$. The cells were collected by centrifugation (5,000 rpm for 10 min) and washed twice with sterile PBS (3.2 mM Na_2HPO_4, 0.5 mM KH_2PO_4, 1.3 mM KCl, and 135 mM NaCl, pH 7.4) followed by resuspension in PBS to $A_{600\ nm} \sim 1.0$.

rhPg Binding to GAS Cells and Activation on Cells—Fifty microliters of $A_{600\ nm} \sim 1.0$ cells prepared as described above were used to coat 96-well Maxisorb plates (Nunc, Thermo Scientific) at 4 °C overnight. Following three washes with PBS, plates were blocked with 200 μl of blocking buffer (1% BSA in PBS) for 2 h at room temperature. The wells were washed as above, and 100 μl of 20 μg/ml rGlu^1-hPg in blocking buffer was added to each well. The rhPg was allowed to bind to the immobilized cells for 2 h at room temperature. After washing with PBS, the following steps were performed for two different assays. For rhPg binding assays, mouse anti-hPg (Enzyme Research Laboratories) in blocking buffer was added, and the mixture was incubated for 2 h at room temperature followed by washing with PBS and incubation with 100 μl of HRP-conjugated goat anti-mouse IgG in blocking buffer for 2 h. After washing as above, the color was developed with the addition of 3,3′,5,5′-tetramethylbenzidene substrate (TMB; R&D Systems, Minneapolis, MN) and measured as the $A_{450\ nm}$. For assays of rhPg activation on cells, 200 μl of 0.25 mM S2251 in 10 mM Hepes, 150 mM NaCl, pH 7.4, was added to each well. The reactions were accelerated with 5 nM rSK, and the amidolytic activity generated by hPm hydrolysis of substrate S2251 was monitored by measuring the $A_{405\ nm}$.

GenBank^{TM} Sequence Accession—The *sk* nucleotide sequences reported herein have been submitted to GenBank^{TM} with accession numbers JX898180 to JX898186.

RESULTS

Phylogenetic Analysis of SK Clusters—According to the published information and the genomic sequences reported (15, 17, 22) GAS strains NS210, NS53, NS931, and NZ131 were chosen to clone the SK1 genes. NS223, NS455, NS88.2, and AP53 were selected to clone the SK2b genes. To study the functional relationships between SK2b and PAM, strain AP53 was selected because of its representative well studied PAM_{AP53} protein (14, 23, 24). The coding sequences for the β-domains of these rSKs (Fig. 1*A*) were aligned and then examined by phylogenetic analysis (Fig. 1*B*). Amino acid sequence alignments of the β-domains revealed that the protein sequences were relatively conserved (88–98% identities, shown as *red*, *blue*, and *black letters* in Fig. 1*A*) within the same SK cluster but showed significant differences between the SKs of cluster 1 and cluster 2b (60–63% identities; shown as *red* in Fig. 1*A*). Although there is little information available regarding the residues that play important roles in the functional differences between cluster 1 and cluster 2b SKs, the residues (shown as *black asterisks* in Fig. 1*A*), that are conserved in one cluster but are significantly different between clusters are candidates for further study.

As expected, *sk* genes from strains NS210, NS53, NS931, and NZ131 fell within cluster 1, whereas those from NS223, NS455, and NS88.2 belong to cluster 2b. Although the *sk* gene from AP53 has not been reported, it is not surprising to find that it belongs to cluster 2b on the basis of the significant coinheritance between *pam* and *sk2b* genes in GAS strains (16).

hPg Activation by Purified Cluster 1 SKs and Cluster 2b SKs—To study the hPg activation characteristics of these rSK variants, the *sk* genes cloned from eight GAS strains were expressed in *E. coli* and purified (supplemental Fig. 1), without any nonnative residues. The purified proteins contained 414 residues, encompassing residues 27–440 of each SK. The consistency between the experimental molecular weights and calculated molecular weights of the final products of each protein was further confirmed by MALDI-TOF, and all were within 0.5% of the calculated values (supplemental Table 2).

With these purified rSKs, their ability to stimulate activation of rGlu^1-hPg was determined in a continuous assay by measuring the amidolytic activities generated by the forming hPm. A striking difference in hPg activation capacities was displayed by rSKs from the two different clusters (Fig. 2*A*). All cluster 1 SKs (rSK_{NS210}, rSK_{NS53}, rSK_{NS931}, and rSK_{NZ131}) activated rGlu^1-hPg efficiently to hPm, as reflected by the fast increase of $A_{405\ nm}$ forming from amidolysis of S2251 by hPm. In contrast, assays with all cluster 2b SKs (rSK_{AP53}, rSK_{NS223}, rSK_{NS455}, and $rSK_{NS88.2}$) showed development of only a slight increase in $A_{405\ nm}$ after 60 min, indicating that little hPm was produced. Because in these assays the $A_{405\ nm}$ reflects not only the activation rate of hPg to hPm but also the amidolytic activity of the continuously forming hPm, more quantitative estimates of the comparative rSK activities were determined from the $A_{405\ nm}$ *versus* t^2 plots (Fig. 2*B*), where the slopes of these lines were calculated and compared (Fig. 2*C*). Although there were small differences in the rates of the SKs in the same cluster, in general, the rates of cluster 1 SKs were at least ~13–25-fold higher (0.78–1.56 m$A_{40\ nm}$ min^{-2}) than those of cluster 2b SKs (0.03–0.06 m$A_{405\ nm}$ min^{-2}).

Binding of SK to Glu^1-hPg—According to the proposed mechanism for hPg activation by SK, these proteins must first interact to form a stoichiometric complex. This is followed by conformational and structural transformations to form the hPg activator SK-hPm (13). As the first step of this process, binding

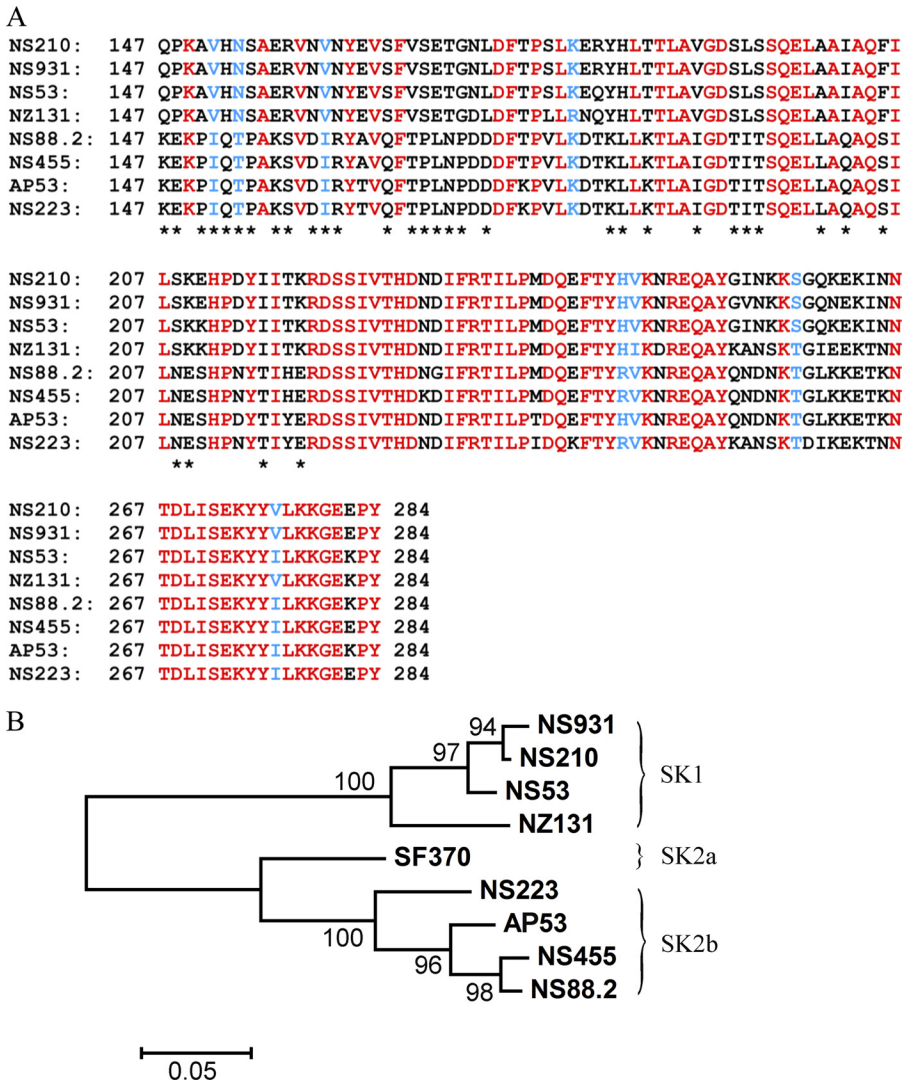

FIGURE 1. **Evolutionary properties of rSKs from GAS strains.** *A*, amino acid sequence alignments of rSKs cloned in this study. The nucleotide sequences obtained were translated into amino acid sequences, and residues 1–414 of these translated sequences were aligned by ClustalX (41). Only the β-domains (amino acids 147–284) are shown. Strictly conserved residues in all eight SKs are colored *red*, and conservatively substituted residues in all eight SKs are *blue*. The residues that are strictly conserved in one cluster and are different between clusters are indicated by *asterisks*. *B*, phylogenetic tree for a 423-bp (nucleotide positions 517–939, corresponding to amino acids 147–287) variable region encoding the SK β-domain of the eight SKs cloned in this study. The sequence of a known cluster, 2a SF370-SK_{SF370}, was obtained from online genomic sequence data and is included here as an outlier compared with cluster 1 and cluster 2b SKs. The tree was constructed by the neighbor-joining method using MEGA, version 4.1 (42). Bootstrap values (500 replicates) are indicated at the nodes. *Scale bar* = 0.05 substitutions per site. Cluster designations are indicated.

of hPg by SK undoubtedly plays an important role in the activation. To determine whether there is a difference in hPg binding abilities between cluster 1 SKs and cluster 2b SKs, which could be a factor in the weaker activation of hPg by SK2b, SPR was applied to investigate the binding affinities of hPg to these SK variants. Here, a Glu^1-hPg mutant, rGlu^1-hPg[S741A], in which the active site Ser^{741} was replaced with Ala, was used to avoid activation of WT hPg during the binding process. Examples of the data obtained are shown in Fig. 3 for a typical SK1 (Fig. 3*A*, rSK_{NS53}) and SK2b (Fig. 3*B*, rSK_{NS223}), and all of the binding data are listed in Table 1. Sensorgrams similar to that of rSK_{NS53} (Fig. 3*A*) were observed for the other three rSK1 proteins (rSK_{NS210}, rSK_{NS931},and rSK_{NZ131}), whereas sensorgrams of the additional three rSK2b proteins (rSK_{AP53}, rSK_{NS455}, and $rSK_{NS88.2}$) were similar to that of rSK_{NS223} (Fig. 3*B*). The 1:1 binding model from Biacore X100 Evaluation software gave good fits for all of these sensorgrams (sensorgrams ($\chi^2 < 2\%$ R_{max}). By comparing these results, the rSK1 displayed both faster association (20–168-fold faster) and disassociation (1.5–4.8-fold faster) rates than the SK2b.

A good correlation is seen between the capabilities of SK to bind hPg and to activate hPg. Within the same cluster, the SK that shows higher hPg binding ability also activates hPg more efficiently. The only exception is $rSK_{NS88.2}$, which shows tighter hPg binding (202 nM) than the other rSK2b proteins (321, 255, and 232 nM for rSK_{AP53}, rSK_{NS233}, and rSK_{NS455}, respectively) but has a lower hPg activation activity (0.03 $mA_{405\ nm}\ min^{-2}$) than rSK_{NS455} (0.06 $mA_{405\ nm}\ min^{-2}$). However, as a whole, the affinities of rSK2b proteins (202–321 nM) for hPg are much lower than those of rSK1 proteins (5–24 nM), which is in good agreement with the difference in hPg activation abilities between cluster 1 SKs and cluster 2b SKs. These results sug-

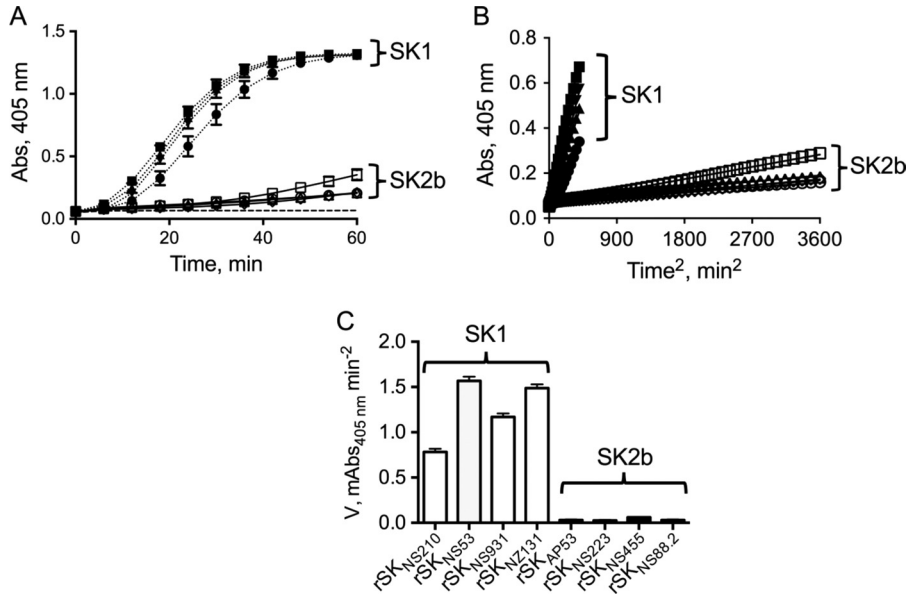

FIGURE 2. **Activation of rGlu[1]-hPg by purified rSKs.** *A*, activation of 0.2 μM of rGlu[1]-hPg by 5 nM of purified cluster 1 SKs (rSK$_{NS210}$ (●), rSK$_{NS53}$ (■), rSK$_{NS931}$ (▲), and rSK$_{NZ131}$ (▼) with *dashed lines*) and cluster 2b SKs (rSK$_{AP53}$ (◇), rSK$_{NS223}$ (○), rSK$_{NS455}$ (□), and rSK$_{NS88.2}$ (△) with *solid lines*) were measured using one-stage activation assays in 10 mM Hepes/150 mM NaCl, pH 7.4. The control without rSK (*dashed line* without symbols) was performed under the same conditions except without the addition of SK. The generation of amidolytic activity was monitored continuously by the absorbance (*Abs*) at 405 nm *versus* time at 37 °C using S2251 (*H*-D-Val-Leu-Lys-pNA·2 HCl). *B*, $A_{405\ nm}$ *versus* t^2 transformed from *A* and linear regression of the linearized region. *C*, the initial velocity (*V*) for each strain was obtained from the linear regions of plots of m$A_{405\ nm}$ *versus* t^2.

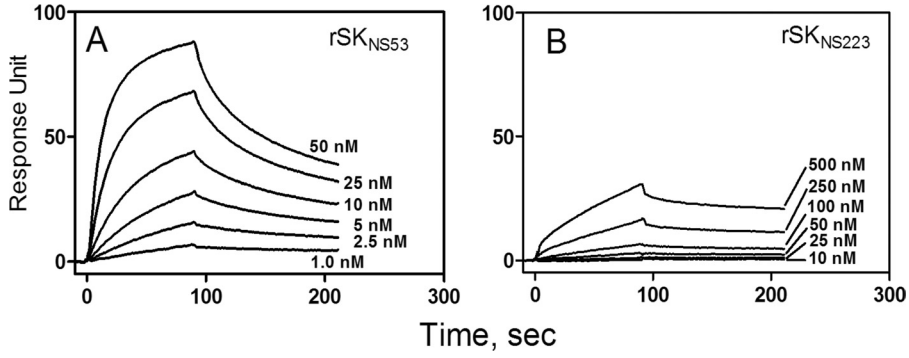

FIGURE 3. **Binding of rSKs to rGlu[1]-hPg[S741A].** Representative SPR sensorgrams for one SK1 (rSK$_{NS53}$) and one SK2b (rSK$_{NS223}$) are presented. The lines within each *panel* represent the binding of the indicated concentrations of rSK$_{NS53}$ (*A*) and rSK$_{NS223}$ (*B*) to immobilized rGlu[1]-hPg[S741A] on a CM5 chip. The sensorgrams shown were generated by subtraction of the nonspecific refractive index component from the total binding. Independent duplicate experiments were also performed with rSK$_{NS210}$, rSK$_{NS931}$, rSK$_{NZ131}$, rSK$_{AP53}$, rSK$_{NS455}$, and rSK$_{NS88.2}$. CM-5 chips were coupled with 1000 RU of rGlu1-Pg[S741A] and used with all four rSK1 protein binding experiments. Another CM-5 chip, coupled with 1500 RU of rGlu1-Pg[S741A], was used for all rSK2b protein binding experiments.

TABLE 1
Binding of rhPg[S741A] to rSK by SPR

SK source	Cluster	k_{on} ($\times 10^4$)	k_{off} ($\times 10^{-3}$)	K_D
		$M^{-1}\ s^{-1}$	s^{-1}	nM
SK$_{NS210}$	C1	30.2 ± 0.07	7.37 ± 0.12	24
SK$_{NS53}$	C1	118.4 ± 0.9	6.16 ± 0.05	5
SK$_{NS931}$	C1	37.5 ± 0.03	4.67 ± 0.06	12
SK$_{NZ131}$	C1	101.8 ± 2.4	8.7 ± 0.18	9
SK$_{AP53}$	C2b	0.70 ± 0.03	2.46 ± 0.09	321
SK$_{NS223}$	C2b	0.70 ± 0.05	1.78 ± 0.08	255
SK$_{NS455}$	C2b	1.32 ± 0.10	3.06 ± 0.15	232
SK$_{NS88.2}$	C2b	1.55 ± 0.05	3.14 ± 0.14	202

gested that the lower affinity of cluster 2b SKs in complexes with hPg is the basis for their lower activation of hPg.

Effects of hFg and M Proteins on hPg Activation by SKs—Because cluster 2b SKs show much weaker activation of hPg compared with cluster 1 SKs, other factors must enable the activation of hPg by SK2b, as it is documented that GAS cells that express SK2b can obtain cell-bound hPm, even to a higher level than those GAS cells expressing SK1 (17). Two hPg-binding proteins, hFg and PAM, which play important roles in GAS pathogenesis (5, 7, 9), had been studied previously with GAS crude culture supernates that contained SK (17) but failed to reveal any function of PAM on hPg activation by cluster 2b SKs. However, considering the possible effects of the numerous ingredients in culture supernates that were used in that study, especially the presence of the antifibrinolytic agent, L-lysine, we reexamined the functions of hFg and PAM on hPg activation by different SKs using purified systems to eliminate considerations of media components that exist in crude assays. In this context, PAM$_{AP53}$ protein, which is well known for its high binding affinity to hPg (14), was used.

In addition to investigating the role of hFg and PAM on hPg activation in this system, the effects of another M protein, M1$_{SF370}$, which shows structure and anti-phagocytic functions similar to those of PAM$_{AP53}$, but does not possess direct hPg

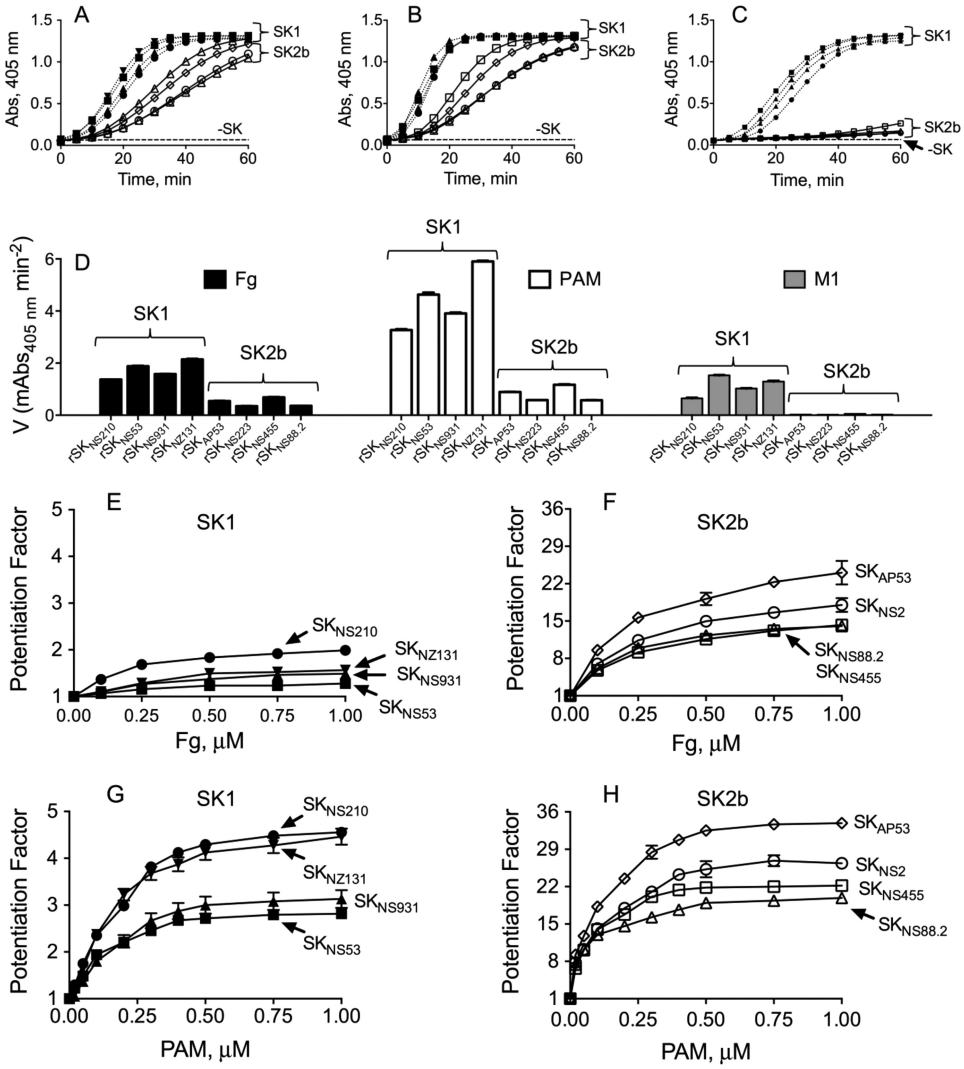

FIGURE 4. **Effects of hFg, PAM_{AP53}, or $M1_{SF370}$ on the activation of $rGlu^1$-hPg by purified rSK.** *A–C*, 0.5 μM hFg (*A*), 0.5 μM PAM_{AP53} (*B*), or 0.5 μM $M1_{SF370}$ (*C*) was premixed with $rGlu^1$-hPg and S2251 in 10 mM Hepes/150 mM NaCl, pH 7.4. After the addition of 5 nM SK, the absorbance (*Abs*) at 405 nm was measured at 1-min intervals. ●, rSK_{NS210}; ■, rSK_{NS53}; ▲, rSK_{NS931}; ▼, rSK_{NZ131}; ◇, rSK_{AP53}; ○, rSK_{NS223}; □, rSK_{NS455}; △, $rSK_{NS88.2}$. *D*, the initial velocity (*V*) as $mA_{405\ nm}\ min^{-2}$ was calculated from the slopes of the plot of $A_{40\ nm}$ *versus* t^2. *E–H*, effects of different concentrations of hFg or PAM_{AP53} (0–1 μM) were measured with SK1 (*E* and *G*) and SK2b (*F* and *H*) as labeled. The ratio of initial velocity in the presence and absence of hFg or PAM_{AP53} was defined as the potentiation factor.

binding ability (25, 26), was also studied in parallel with PAM_{AP53}. Compared with the results in the absence of either hFg or PAM_{AP53} (Fig. 2*A*), the presence of both hFg (Fig. 4, *A* and *D*) and $rPAM_{AP53}$ (Fig. 4, *B* and *D*) clearly stimulated $rGlu^1$-hPg activation of both SK1 and SK2b. The activation rates by cluster 1 SKs increased 1.2–1.8-fold and 2.7–4.2-fold in the presence of 0.5 μM hFg (Fig. 4, *D* and *E*) and 0.5 μM $rPAM_{AP53}$ (Fig. 4, *D* and *G*), respectively. More significantly, the stimulation of these activation rates by cluster 2b SKs increased 10–18-fold and 17–30-fold in the presence of 0.5 μM hFg (Fig. 4, *D* and *F*) and 0.5 μM PAM_{AP53} (Fig. 4, *D* and *H*), respectively. Further investigation revealed that the stimulatory effects of both hFg (Fig. 4, *E* and *F*) and $rPAM_{AP53}$ (Fig. 4, *G* and H) on all of these SKs were concentration-dependent. Contrary to the stimulation by hFg and PAM_{AP53}, $M1_{SF370}$ did not show any stimulatory effect on $rGlu^1$-hPg activation by either cluster 1 or cluster 2b SKs (Fig. 4, *C* and *D*) compared with the results obtained in its absence, when $M1_{SF370}$ was used in place of PAM_{AP53}.

Effects of Parent Cells on hPg Activation by SKs—The above results showed that PAM_{AP53} enabled cluster 2b SKs to significantly stimulate activation of hPg, whereas cluster 1 SKs did not display this effect to nearly the same extent. To determine whether the strains used had important hPg-binding proteins with a role similar to that of PAM_{AP53}, and whether the nature of the secreted SK reflected the ability of hPg to bind to these cells, hPg binding studies were conducted on cells of these strains. As shown by the sandwich ELISAs, cells of all cluster 2b SK-expressing strains showed a high hPg binding capacity similar to cells of the AP53 strain. Cells of all cluster 1 SK-expressing strains displayed more than 5-fold lower hPg binding affinities (Fig. 5*A*).

Additional enzymatic assays revealed that barely detectable hPm activity was seen on the cells of cluster 1 SK-expressing strains (Fig. 5*B*), in agreement with the lack of strong binding ability of hPg cluster 1 SK-expressing cells. In contrast, high hPm activities were obtained on cluster 2b SK-expressing cells

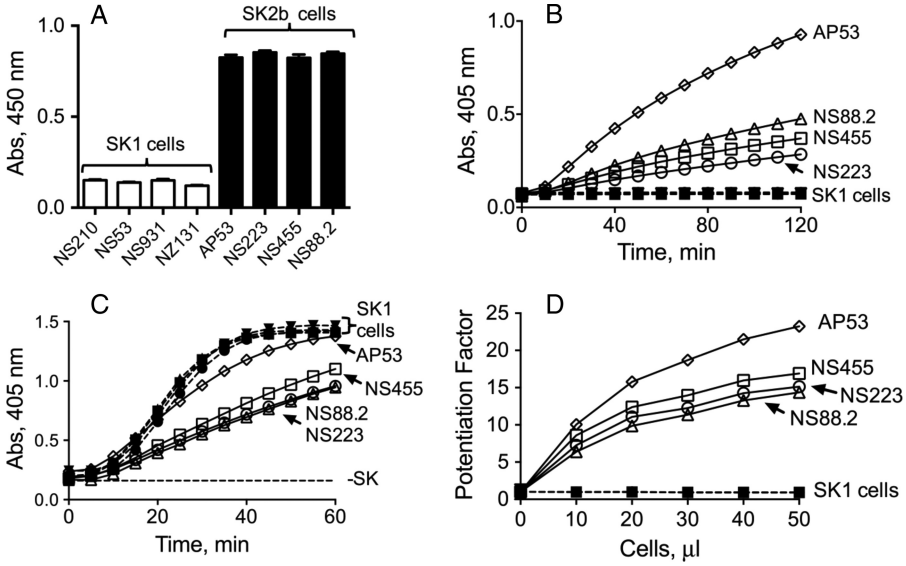

FIGURE 5. **hPg binding ability of GAS strains and effects of GAS cells.** *A*, the rhPg binding ability of GAS strains that produce the corresponding SKs were studied. Cells were bound to microtiter plates, and the bound cells were incubated with rGlu[1]-hPg. The cell-bound Glu[1]-hPg was detected by ELISA with appropriate antibodies. *B*, activation of hPg on GAS cells. GAS cells were bound to microtiter plates and incubated with Glu[1]-hPg. The activation of bound rGlu[1]-hPg was detected by the addition of S2251 and the corresponding rSK. SK1 expression cells (with *dashed lines*): ●, NS210; ■, NS53; ▲, NS931; and ▼, NZ131. SK2b expression cells (with *solid lines*): ◇, AP53SK; ○, NS223; □, NS455; and △, NS88.2. *C*, activation of Glu[1]-hPg in the presence of 50 μl of GAS cells ($A_{600\ nm}$, 1.0). The GAS cell suspension, along with rGlu[1]-hPg and S2251, was mixed in a microtiter plate well, and the assay was accelerated by the addition of the corresponding rSK, and the absorbance (*Abs*) at 405 nm was measured at 1-min intervals. *D*, effects of different amounts of GAS cells on rGlu[1]-hPg activation by the corresponding rSKs. The assays were performed as described in *C* with different volumes of cells, and the potentiation factors were calculated by the ratio of initial velocity in the presence and absence of GAS cells.

(Fig. 5*B*), again reflective of the tight binding of hPg and hPm to PAM-like proteins on these cells. Further, when cells were added to the hPg activation assays, cluster 1 SKs showed the same rates either in the presence (Fig. 5*C*) or absence (Fig. 2*A*) of their parent cells, regardless of the amount of cells added (Fig. 5*D*). However, with the addition of 50 μl of their parent cells, cluster 2b SKs produced more than 10-fold higher amounts of hPm activity (Fig. 5, *C* and *D*) compared with that in the absence of cells, and the rates of Glu[1]-hPg activation increased in proportion to the amount of cells added, until saturation was achieved (Fig. 5*D*). These results demonstrated that SK2b-expressing cells possess an important hPg-binding protein with properties very similar to purified PAM and have a factor that strongly stimulates hPg activation by their daughter SKs. On the contrary, SK1-expressing cells do not produce this hPg-binding protein and, correspondingly, do not stimulate hPg activation by their respective SK1 proteins.

Studies with Mutant GAS Lines—To mechanistically address whether PAM is the critical hPg-binding protein in cluster 2b SK-expressing strains, which binds and correspondingly stimulates hPg activation by cluster 2b SKs, three GAS mutant strains were employed. AP53/Δ*pam*, which is an AP53 mutant with the open reading frame of *pam* in strain AP53 replaced in-frame by the *cat* gene, and NS88.2/*prp*, which is a NS88.2 mutant strain, with four amino acid residues (Lys[96], Lys[101], Arg[107], and His[108]) that are critical for hPg binding in its PAM-related protein (Prp), converted to codons for Ala (27) lost most of their hPg binding ability (Fig. 6*A*). The residual hPg binding abilities of these two mutant strains were only comparable to those of the cluster 1 SK-expressing strains, and the bound hPg could not be activated by their daughter SKs, *viz.* SK_{AP53} and $SK_{NS88.2}$ (Fig. 6*B*). NS88.2/*prpRC*, which has the mutated *prp*

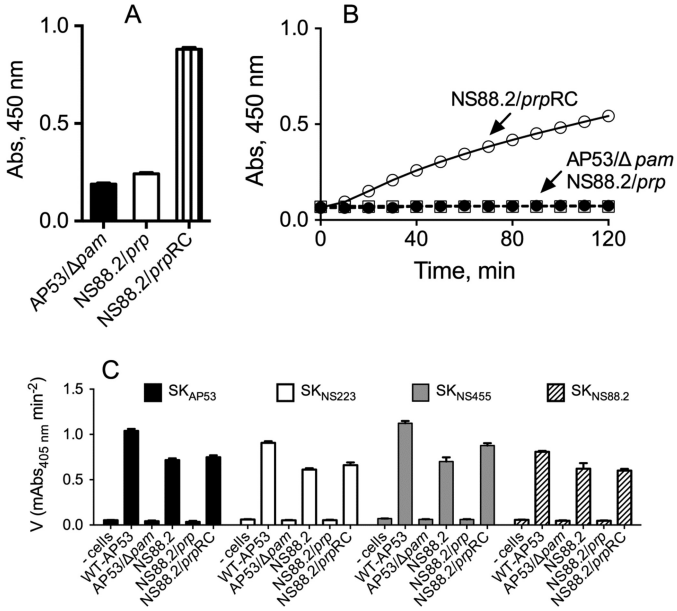

FIGURE 6. **hPg-binding ability of GAS hPg-binding protein mutants and effects of these cells on activation of rGlu[1]-Pg by SK2b.** *A*, rGlu[1]-hPg binding to mutant cells: AP53/Δ*pam*, NS88.2/*prp*, and NS88.2/*prp*RC. *B*, rGlu[1]-hPg activation on the following cells: AP53/Δ*pam* (□); NS88.2/*prp* (●); and NS88.2/*prp*RC (○). *C*, rGlu[1]-hPg activation in the presence of 50 μl of WT and mutant AP53 and NS88.2 cells ($A_{600\ nm} \sim 1.0$) by SK2b.

residues reverse-complemented (RC) to the WT sequence, showed as high hPg binding, as the WT NS88.2 strain and the bound hPg were highly activatible by $rSK_{NS88.2}$ (Fig. 6*B*).

The effects of these three mutant strains as well as WT AP53 and WT NS88.2 on hPg activation by cluster 2b SKs were investigated by including these cell lines in the activation assays. The results (Fig. 6*C*) showed that WT AP53 cells highly stimulated

hPg activation by rSK_{AP53}, whereas AP53/Δ*pam* lost all of its stimulatory effects. These results strongly suggest that PAM is the only hPg-binding protein on AP53 GAS cells that enables hPg activation by its SK2b. Similarly, in the case of $rSK_{NS88.2}$, WT NS88.2 cells showed high stimulatory effects, whereas the *pam* mutant with the hPg binding site ablation NS88.2/*prp* lost all of its stimulatory effects of $rSK_{NS88.2}$ on hPg activation. When the hPg binding sites were reverse-complemented in the mutant NS88.2/*prp*RC, complete stimulatory function was regained. These results clearly showed that the hPg binding function of Prp in the PAM-related GAS cell strain NS88.2 is the factor that stimulates the activation of hPg with SK2b. The same results were obtained when using these WT and mutant strains with other SK2bs in this study (Fig. 6*C*). Combined with the data showing that all of these SK2b-expressing cells have PAM or PAM-related hPg-binding proteins, we concluded that all of these SK2b-expressing cells employ the same strategy to stimulate the SK that they express.

DISCUSSION

For many years, most functional studies with SK focused on SKg from *Streptococcus dysgalactiae* sub. *equismilis* (13, 28–30), which most resembles a GAS subcluster 1 SK. Although very important mechanistic information on hPg activation has been obtained from much work with SKg, new aspects of SK structure-function relationships have emerged with data showing that very important, but subtle, aspects of the mechanism of SK activation of hPg may have evolved in conjunction with the infective nature of the bacterium in which it is expressed. Recent studies have strongly indicated that there are evolutionary and functional differences among the GAS SKs, and these differences now allow a new focus on SKs from this bacterium because of its numerous strains and the different properties of the SKs produced in these strains. In fact, a strong coinheritant relationship between specific virulence-determining M proteins (*e.g.* PAM) and cluster 2b SKs has been suggested (16). If in fact confirmed, this combination of genes allows direct high affinity binding of hPg and hPm to the surface of certain strains of GAS cells that are skin-tropic and highly invasive. Although superficial GAS infections by many strains are easily treatable with antibiotic therapy, a subclass of pharynx and skin infections, with GAS strains that directly or indirectly bind host plasminogen and plasmin, can be highly invasive and very difficult to treat (*e.g.* necrotizing fasciitis) with potential lethal consequences.

A recent study demonstrates a striking difference in hPg activation capacities by SKs from the two different clusters, cluster 1 and cluster 2b (17). With the sk1 allele, high levels of SK activity were detected, whereas no SK activity was found in culture supernates of strains that harbor the sk2b allele. A similarly interesting result was also observed in our current study, wherein low activities were observed for SK2b. Both studies showed that hFg stimulated the activities of both cluster 1 and cluster 2b SKs, and PAM stimulated the activities of cluster 1 SKs. However, dramatically different results were shown when the effects of PAM protein on the activities of cluster 2b SKs were studied. No stimulation was observed with the addition of PAM when culture supernates were used as the source of SK in

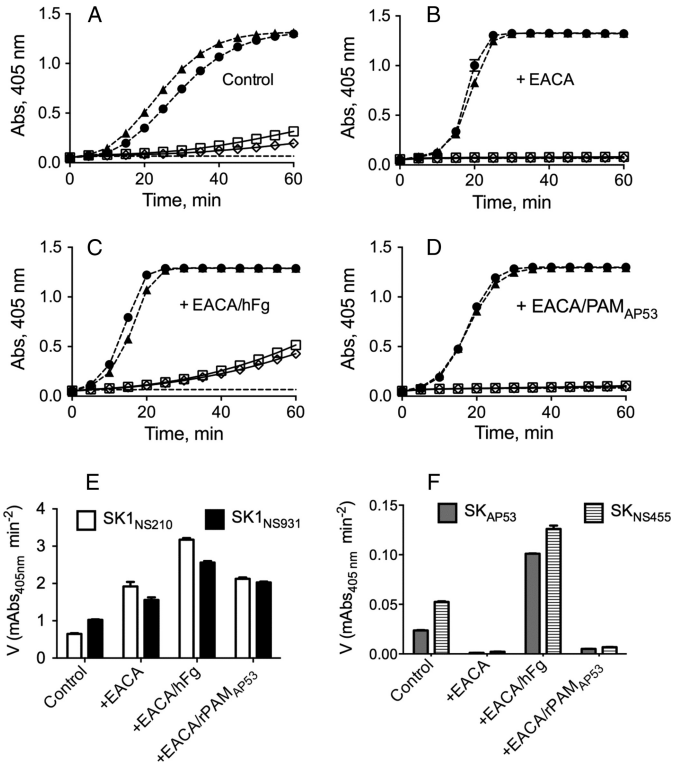

FIGURE 7. **Effects of EACA and hFg or EACA and PAM_{AP53} on hPg activation by SK.** SK1 (with *dashed lines*): rSK_{NS210} (●); rSK_{NS931} (▲). SK2b (with *solid lines*): rSK_{AP53} (◇); rSK_{NS455} (□). EACA (10 mM)/hFg (0.5 μM) or EACA (10 mM)/PAM_{AP53} (0.5 μM) were premixed with rGlu^1-Pg and S2251 in 10 mM Hepes/150 mM NaCl, pH 7.4. After acceleration with 5 nM SK, the $A_{405\,nm}$ was measured at 1-min intervals. Control assays were performed without the addition of EACA, hFg, or PAM_{AP53}. *A*, control assays in the absence of EACA, hFg, or PAM_{AP53}. *B*, hPg activation in the presence of EACA. *C*, hPg activation in the presence of both EACA and hFg. *D*, hPg activation in the presence of both EACA and PAM_{AP53}. *E* and *F*, the data from *A–D* were replotted as initial rates of activation under the above conditions.

the previous work (17), but a strong stimulation effect of PAM was observed when the purified cluster 2b SKs were used in the current study. This leads to completely different conclusions regarding the effects of PAM on the activities of cluster 2b SKs. Specifically, the major differences between the two studies is that the previous investigation used culture supernates as the source of SK (17), and our current work employed purified SKs. It has been shown that L-lysine, as well as many of its analogues (*e.g.* ϵ-aminocaproic acid (EACA)) normally present in culture medium, inhibits SK-hPg activator formation and substrate hPg binding through kringle-dependent mechanisms (31). One explanation for the differences between the previous study and ours is that L-lysine, and perhaps other media components in the supernates, differentially affects activation by cluster 1 and cluster 2b SKs.

To illustrate the importance of this issue, the data from Fig. 7 show the results of the activation of hPg in the presence of the lysine analogue EACA. EACA effectively blocks the activities of cluster 2b SKs (Fig. 7, *B* and *F*) but has little effect on the stimulatory activities toward cluster 1 SKs (Fig. 7, *B* and *E*). With the addition of both EACA and hFg, the activities of cluster 1 SKs were stimulated, and the activities of cluster 2b SKs were rescued and even stimulated (Fig. 7, *C* and *E*). With the addition of both EACA and PAM, however, there was stimulation but no

more than with only EACA for cluster 1 SKs, and still no activity was observed for cluster 2b SKs (Fig. 7, *D* and *E*), likely because of displacement by EACA of the hPg·PAM complex that is needed for SK2b activation (17). This finding is in good agreement with the previous study. Thus, we feel that lysine or lysine analogues in the culture supernatant play an important role when present and could block the activation of hPg by SK2b, with or without PAM.

Whereas cluster 2b SKs displayed weak activation of hPg, the addition of either hFg or PAM_{AP53} led to dramatically enhanced activation rates of Glu^1-hPg. However, the addition of $M1_{SF370}$ did not show an effect on this activation. Considering that both hFg and PAM_{AP53} are well known hPg-binding proteins, whereas $M1_{SF370}$ does not have direct hPg binding ability, we concluded that the binding of hPg by these proteins alters the conformation of hPg and allows faster activation by cluster 2b SKs. We have shown previously that Glu^1-hPg adopts a closed activation-resistant conformation in Cl^--containing buffers and is altered to an open, highly activatible conformation upon occupancy of its kringle lysine-binding sites with lysine-like ligands (32–34). The significantly higher stimulation of Glu^1-hPg activation by SK2b obtained with PAM (17–30-fold) than with hFg (10–18-fold) suggests that the conformational changes in hPg induced by the binding of PAM to kringle-2 of hPg place hPg in a more activatible form for cluster 2b SKs than the conformations induced by the binding of hFg, primarily to kringles 1, 4, and 5 of hPg.

Although the activities of cluster 1 SKs were also stimulated 3–4-fold by PAM, this may not be biologically meaningful, as available knowledge indicates that strains harboring cluster 1 SKs do not contain the *pam* gene (16). It is notable that with the addition of PAM protein, the activities of cluster 2b SKs increase from nearly zero to a level comparable to cluster 1 SKs. Genes expressing PAM-like proteins have been detected and cloned from all four of the cluster 2b SK-expressing strains (14, 35, 36), and we confirmed herein that the proteins express and function well in all of these strains with regard to hPg binding and activation. With detailed activation assays using GAS cells, we have proved that PAM is the factor, and the only factor, on the GAS cell surface to stimulate SK activity via its binding of hPg by the kringle-2 domain. Other hPg receptors (37), such as streptococcal enolase (*sen*) (38) and plasmin receptor protein (*plr*) (39), that exist in GAS cells are apparently not meaningful, at least in PAM-expressing strains. This is shown not only through the use of WT GAS cells, which do not express PAM and do not stimulate hPg activation by the SKs that they produce, but also through inactivation of the *pam*-like gene in SK2b-producing NS88.2 cells, which results in a cell line that is also refractive to stimulation of hPg activation by SK2b (40).

According to the results of this study, two pathways of cell-bound hPm acquisition by different GAS strains expressing SK2b and PAM are proposed (Fig. 8). In one (Fig. 8, *pathway A*), hPg interacts with hFg and becomes activatible by cluster 2b SK. After activation by SK2b, the resulting hPm is acquired by cells through binding of hPm by PAM. In the second, more efficient pathway (Fig. 8, *pathway B*), hPg interacts directly with PAM, which enhances its activation by SK2b. This second pathway is likely the more important one, because we show herein

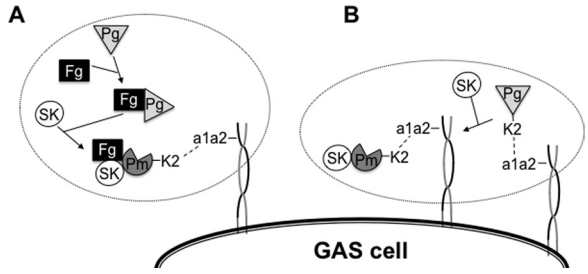

FIGURE 8. **Schematic diagram summarizing the hypothesized pathways of cell surface hPm acquisition by GAS strains expressing SK2b.** Two pathways are proposed. *A*, in the first pathway, hPg binds to hFg to accelerate its activation by SK2b. The resulting hPm is then bound to the cell surface, via its K2 domain by the a1a2 domain of PAM. *B*, in the second pathway, hPg, via its K2 domain, interacts directly with the a1a2 domain of PAM to accelerate its activation by SK2b, and the cells then acquire hPm activity. This figure is modified from Fig. 5 in Ref. 17.

that shows higher activity when hPg is bound to PAM than when bound to hFg. However, in both pathways, PAM is necessary to recruit cell surface hPm. This functional dependence could provide a strong coselective pressure for the PAM and cluster 2b SKs to uniformly exist in skin-tropic invasive GAS strains, thus explaining the coinheritance of these two genes in these strains of GAS.

REFERENCES

1. Carapetis, J. R., Steer, A. C., Mulholland, E. K., and Weber, M. (2005) The global burden of group A streptococcal diseases. *Lancet Infect. Dis.* **5,** 685–694
2. Le Hello, S., Doloy, A., Baumann, F., Roques, N., Coudene, P., Rouchon, B., Lacassin, F., and Bouvet, A. (2010) Clinical and microbial characteristics of invasive *Streptococcus pyogenes* disease in New Caledonia, a region in Oceania with a high incidence of acute rheumatic fever. *J. Clin. Microbiol.* **48,** 526–530
3. Smeesters, P. R., McMillan, D. J., and Sriprakash, K. S. (2010) The streptococcal M protein: a highly versatile molecule. *Trends Microbiol.* **18,** 275–282
4. Beall, B., Facklam, R., and Thompson, T. (1996) Sequencing emm-specific PCR products for routine and accurate typing of group A streptococci. *J. Clin. Microbiol.* **34,** 953–958
5. Bisno, A. L., Brito, M. O., and Collins, C. M. (2003) Molecular basis of group A streptococcal virulence. *Lancet Infect. Dis.* **3,** 191–200
6. Mitchell, T. J. (2003) The pathogenesis of streptococcal infections: from tooth decay to meningitis. *Nat. Rev. Microbiol.* **1,** 219–230
7. Cunningham, M. W. (2008) Pathogenesis of group A streptococcal infections and their sequelae. *Adv. Exp. Med. Biol.* **609,** 29–42
8. Musser, J. M., and Shelburne, S. A. (2009) A decade of molecular pathogenomic analysis of group A *Streptococcus*. *J. Clin. Invest.* **119,** 2455–2463
9. Cole, J. N., Barnett, T. C., Nizet, V., and Walker, M. J. (2011) Molecular insight into invasive group A streptococcal disease. *Nat. Rev. Microbiol.* **9,** 724–736
10. Sun, H., Ringdahl, U., Homeister, J. W., Fay, W. P., Engleberg, N. C., Yang, A. Y., Rozek, L. S., Wang, X., Sjöbring, U., and Ginsburg, D. (2004) Plasminogen is a critical host pathogenicity factor for group A streptococcal infection. *Science* **305,** 1283–1286
11. Walker, M. J., McArthur, J. D., McKay, F., and Ranson, M. (2005) Is plasminogen deployed as a *Streptococcus pyogenes* virulence factor? *Trends Microbiol.* **13,** 308–313
12. Robbins, K. C., Summaria, L., Hsieh, B., and Shah, R. J. (1967) The peptide chains of human plasmin. Mechanism of activation of human plasminogen to plasmin. *J. Biol. Chem.* **242,** 2333–2342
13. Schick, L. A., and Castellino, F. J. (1974) Direct evidence for the generation of an active site in the plasminogen moiety of the streptokinase-human plasminogen activator complex. *Biochem. Biophys. Res. Commun.* **57,** 47–54

14. Berge, A., and Sjöbring, U. (1993) PAM, a novel plasminogen-binding protein from *Streptococcus pyogenes*. *J. Biol. Chem.* **268,** 25417–25424
15. McKay, F. C., McArthur, J. D., Sanderson-Smith, M. L., Gardam, S., Currie, B. J., Sriprakash, K. S., Fagan, P. K., Towers, R. J., Batzloff, M. R., Chhatwal, G. S., Ranson, M., and Walker, M. J. (2004) Plasminogen binding by group A streptococcal isolates from a region of hyperendemicity for streptococcal skin infection and a high incidence of invasive infection. *Infect. Immun.* **72,** 364–370
16. Kalia, A., and Bessen, D. E. (2004) Natural selection and evolution of streptococcal virulence genes involved in tissue-specific adaptations. *J. Bacteriol.* **186,** 110–121
17. McArthur, J. D., McKay, F. C., Ramachandran, V., Shyam, P., Cork, A. J., Sanderson-Smith, M. L., Cole, J. N., Ringdahl, U., Sjöbring, U., Ranson, M., and Walker, M. J. (2008) Allelic variants of streptokinase from *Streptococcus pyogenes* display functional differences in plasminogen activation. *FASEB J.* **22,** 3146–3153
18. Sjögren, J., Okumura, C. Y., Collin, M., Nizet, V., and Hollands, A. (2011) Study of the IgG endoglycosidase EndoS in group A streptococcal phagocyte resistance and virulence. *BMC Microbiol.* **11,** 120
19. Ward, P. N., and Leigh, J. A. (2002) Characterization of PauB, a novel broad-spectrum plasminogen activator from *Streptococcus uberis*. *J. Bacteriol.* **184,** 119–125
20. Iwaki, T., and Castellino, F. J. (2008) A single plasmid transfection that offers a significant advantage associated with puromycin selection in *Drosophila* Schneider S2 cells expressing heterologous proteins. *Cytotechnology* **57,** 45–49
21. Nilsen, S. L., and Castellino, F. J. (1999) Expression of human plasminogen in *Drosophila* Schneider S2 cells. *Protein Expr. Purif.* **16,** 136–143
22. McShan, W. M., Ferretti, J. J., Karasawa, T., Suvorov, A. N., Lin, S., Qin, B., Jia, H., Kenton, S., Najar, F., Wu, H., Scott, J., Roe, B. A., and Savic, D. J. (2008) Genome sequence of a nephritogenic and highly transformable M49 strain of *Streptococcus pyogenes*. *J. Bacteriol.* **190,** 7773–7785
23. Ringdahl, U., Svensson, M., Wistedt, A. C., Renné, T., Kellner, R., Müller-Esterl, W., and Sjöbring, U. (1998) Molecular co-operation between protein PAM and streptokinase for plasmin acquisition by *Streptococcus pyogenes*. *J. Biol. Chem.* **273,** 6424–6430
24. Rios-Steiner, J. L., Schenone, M., Mochalkin, I., Tulinsky, A., and Castellino, F. J. (2001) Structure and binding determinants of the recombinant kringle-2 domain of human plasminogen to an internal peptide from a group A streptococcal surface protein. *J. Mol. Biol.* **308,** 705–719
25. Macheboeuf, P., Buffalo, C., Fu, C. Y., Zinkernagel, A. S., Cole, J. N., Johnson, J. E., Nizet, V., and Ghosh, P. (2011) Streptococcal M1 protein constructs a pathological host fibrinogen network. *Nature* **472,** 64–68
26. Lauth, X., von Köckritz-Blickwede, M., McNamara, C. W., Myskowski, S., Zinkernagel, A. S., Beall, B., Ghosh, P., Gallo, R. L., and Nizet, V. (2009) M1 protein allows group A streptococcal survival in phagocyte extracellular traps through cathelicidin inhibition. *J. Innate Immun.* **1,** 202–214
27. Sanderson-Smith, M. L., Dinkla, K., Cole, J. N., Cork, A. J., Maamary, P. G., McArthur, J. D., Chhatwal, G. S., and Walker, M. J. (2008) M protein-mediated plasminogen binding is essential for the virulence of an invasive *Streptococcus pyogenes* isolate. *FASEB J.* **22,** 2715–2722
28. Castellino, F. J., Sodetz, J. M., Brockway, W. J., and Siefring, G. E. (1976) Streptokinase. *Methods Enzymol.* **45,** 244–257
29. Boxrud, P. D., and Bock, P. E. (2000) Streptokinase binds preferentially to the extended conformation of plasminogen through lysine binding site and catalytic domain interactions. *Biochemistry* **39,** 13974–13981
30. Loy, J. A., Lin, X., Schenone, M., Castellino, F. J., Zhang, X. C., and Tang, J. (2001) Domain interactions between streptokinase and human plasminogen. *Biochemistry* **40,** 14686–14695
31. Lin, L. F., Houng, A., and Reed, G. L. (2000) Epsilon amino caproic acid inhibits streptokinase-plasminogen activator complex formation and substrate binding through kringle-dependent mechanisms. *Biochemistry* **39,** 4740–4745
32. Violand, B. N., Sodetz, J. M., and Castellino, F. J. (1975) The effect of ϵ-amino caproic acid on the gross conformation of plasminogen and plasmin. *Arch. Biochem. Biophys.* **170,** 300–305
33. Chibber, B. A., and Castellino, F. J. (1986) Regulation of the streptokinase-mediated activation of human plasminogen by fibrinogen and chloride ions. *J. Biol. Chem.* **261,** 5289–5295
34. Chibber, B. A., Radek, J. T., Morris, J. P., and Castellino, F. J. (1986) Rapid formation of an anion-sensitive active site in stoichiometric complexes of streptokinase and human [Glu1]plasminogen. *Proc. Natl. Acad. Sci., U.S.A.* **83,** 1237–1241
35. Svensson, M. D., Sjöbring, U., and Bessen, D. E. (1999) Selective distribution of a high-affinity plasminogen-binding site among group A streptococci associated with impetigo. *Infect. Immun.* **67,** 3915–3920
36. Sanderson-Smith, M. L., Walker, M. J., and Ranson, M. (2006) The maintenance of high affinity plasminogen binding by group A streptococcal plasminogen-binding M-like protein is mediated by arginine and histidine residues within the a1 and a2 repeat domains. *J. Biol. Chem.* **281,** 25965–25971
37. D'Costa, S. S., Wang, H., Metzger, D. W., and Boyle, M. D. (1997) Group A streptococcal isolate 64/14 expresses surface plasmin-binding structures in addition to Plr. *Res. Microbiol.* **148,** 559–572
38. Pancholi, V., and Fischetti, V. A. (1998) α-Enolase, a novel strong plasmin(ogen)-binding protein on the surface of pathogenic streptococci. *J. Biol. Chem.* **273,** 14503–14515
39. Lottenberg, R., Broder, C. C., Boyle, M. D., Kain, S. J., Schroeder, B. L., and Curtiss, R. (1992) Cloning, sequence analysis, and expression in *Escherichia coli* of a streptococcal plasmin receptor. *J. Bacteriol.* **174,** 5204–5210
40. Sanderson-Smith, M. L., Dowton, M., Ranson, M., and Walker, M. J. (2007) The plasminogen-binding group A streptococcal M protein-related protein Prp binds plasminogen via arginine and histidine residues. *J. Bacteriol.* **189,** 1435–1440
41. Larkin, M. A., Blackshields, G., Brown, N. P., Chenna, R., McGettigan, P. A., McWilliam, H., Valentin, F., Wallace, I. M., Wilm, A., Lopez, R., Thompson, J. D., Gibson, T. J., and Higgins, D. G. (2007) Clustal W and Clustal X version 2.0. *Bioinformatics* **23,** 2947–2948
42. Tamura, K., Dudley, J., Nei, M., and Kumar, S. (2007) MEGA4: Molecular Evolutionary Genetics Analysis (MEGA) software version 4.0. *Mol. Biol. Evol.* **24,** 1596–1599